Electronic Supplementary Material (ESI) for Physical Chemistry Chemical Physics.
This journal is © the Owner Societies 2022

Supplementary Information

Physico-geometrical kinetics of the thermal dehydration of sodium carbonate monohydrate as a compacted composite of inorganic hydrate comprising crystalline particles and matrix

Yuto Zushi, Shun Iwasaki, and Nobuyoshi Koga*

Department of Science Education, Division of Educational Sciences, Graduate School of Humanities and Social Sciences, Hiroshima University, 1-1-1 Kagamiyama, Higashi-Hiroshima 739-8524, Japan

Contents

* Corresponding author; e-mail: nkoga@hiroshima-u.ac.jp

S1. Sample characterization

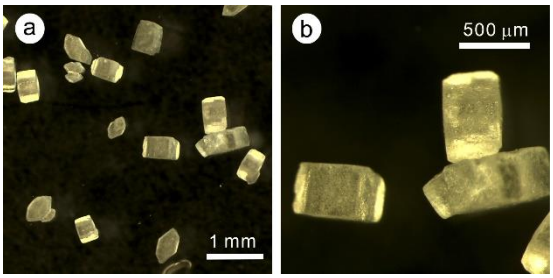

Figure S1. Appearance of the sample particles.

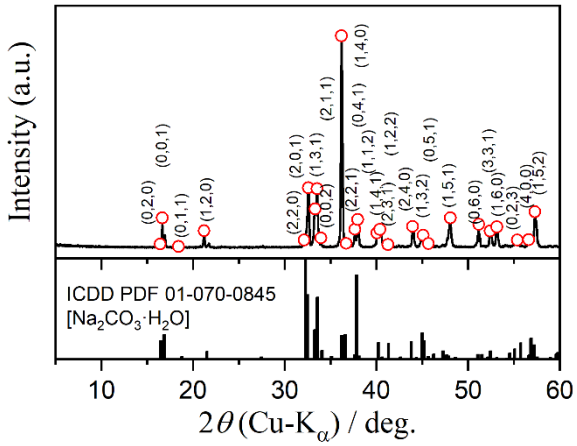

Figure S2. XRD pattern of the sample.

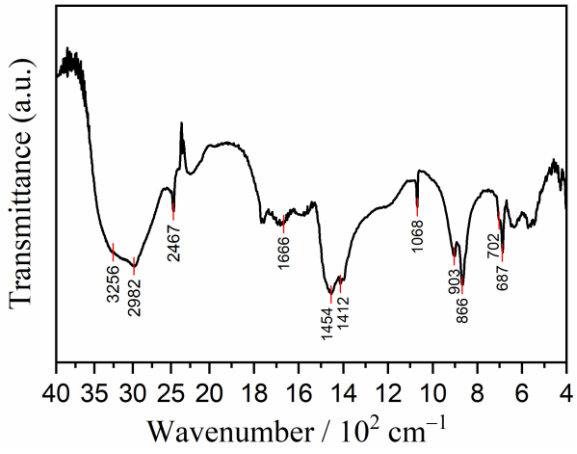

Figure S3. FTIR spectrum of the sample.

Table S1. Assignments of the IR absorption peaks

Peak position /cm^{-1}	Vibration mode
3256	ν_s (O–H)
2982	$2\nu_4$ (CO_3^{2-})
2467	$\nu_1 + \nu_4$ (CO_3^{2-})
1666	bending (O–H)
1500–1400	ν_3 (CO_3^{2-})
1068	ν_1 (CO_3^{2-})
866	ν_2 (CO_3^{2-})
702, 687	ν_4 (CO_3^{2-})

S2. Thermal dehydration behavior

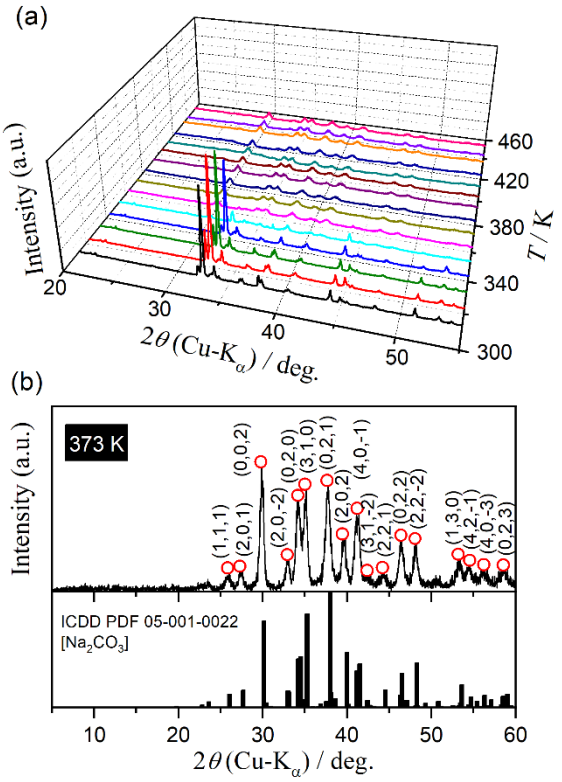

Figure S4. Changes in the XRD pattern of the sample during stepwise isothermal heating: XRD patterns at (a) various temperatures and (b) 373 K.

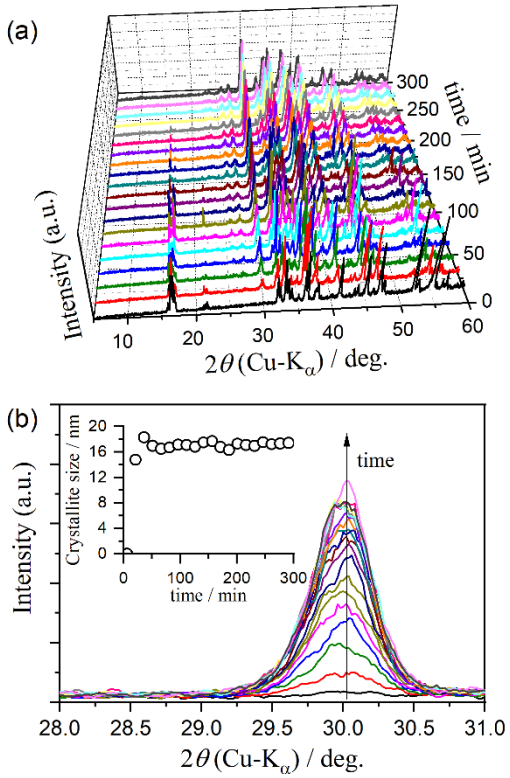

Figure S5. Changes in the XRD patterns of the sample during the isothermal heating at 343 K: (a) XRD patterns at different heating times and (b) changes in the diffraction peak assigned to (0, 0, 2) and the crystallite size of Na_2CO_3 in relation to heating time.

S3. Kinetic analysis

S3-1. Formal kinetic analysis

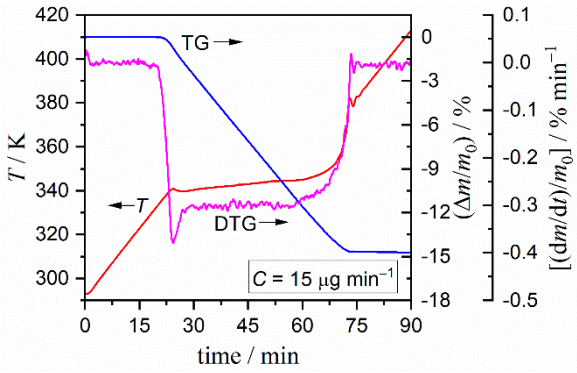

Figure S6. A typical CRTA record for the thermal dehydration of SC-MH (m_0 = 5.02 mg) recorded at C = 15 μg min^{-1} under dry N_2 gas flow (q_v = 300 cm^3 min^{-1}).

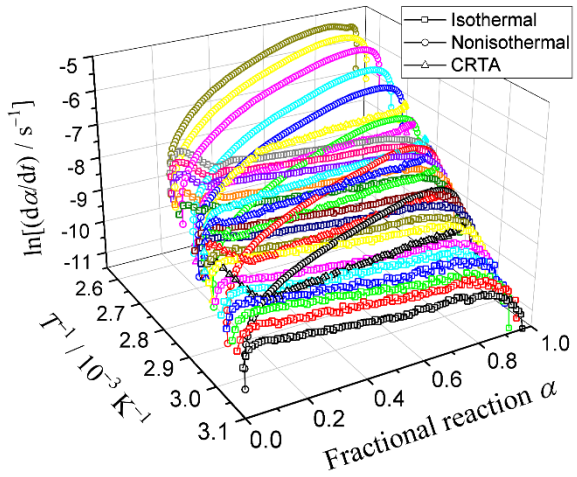

Figure S7. Kinetic data for the thermal dehydration of SC-MH under dry N_2 gas flow recorded under isothermal, linear nonisothermal, and CRTA conditions.

S3-2. Morphological changes during the thermal dehydration

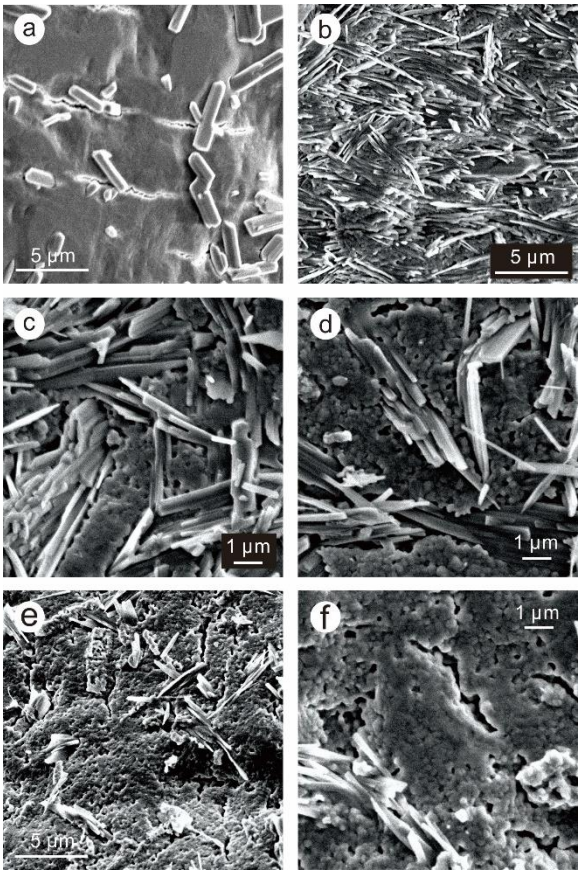

Figure S8. SEM images of the sample surface recorded by ex situ observation for the sample thermally treated by heating to different temperatures at a β of 5 K min^{-1} under dry N_2 gas flow: (a) T = 339 K (α = 0.02), (b) T = 348 K (α = 0.04), (c) T = 349 K (α = 0.04), (d) T = 355 K (α = 0.12), (e) T = 373 K (α = 0.70), and (f) T = 390 K (α =1.00).

S3-3. Mathematical deconvolution analysis

■ Weibull Function

$$y = a_0\left(\frac{a_3-1}{a_3}\right)^{\frac{1-a_3}{a_3}}\left\{\frac{x-a_1}{a_2}+\left(\frac{a_3-1}{a_3}\right)^{\frac{1}{a_3}}\right\}^{a_3-1}\exp\left[-\left\{\frac{x-a_1}{a_2}+\left(\frac{a_3-1}{a_3}\right)^{\frac{1}{a_3}}\right\}^{a_3}+\frac{a_3-1}{a_3}\right] \quad \text{(S1)}$$

Figure S9 shows the results of the MDA applied to the DTG curves for the thermal dehydration of $Na_2CO_3{\cdot}H_2O$ at different β values under dry N_2 gas flow. Irrespective of the β value, the overall DTG peak was successfully deconvoluted into two partially overlapping peaks using the Weibull functions. Also, the contributions (c_i) of each reaction step was calculated from the peak areas were also invariant over the process at different β values. The average c_i values are listed in Table S2. The kinetic curves for each reaction step at different β values were calculated from the mathematically separated DTG peaks as shown in Figure S10. The kinetic curves for each reaction step were subjected to a formal kinetic analysis via the Friedman plot and subsequent master plot method (Figure S11). The kinetic parameters obtained by the kinetic analysis based on the MDA are listed in Table S2.

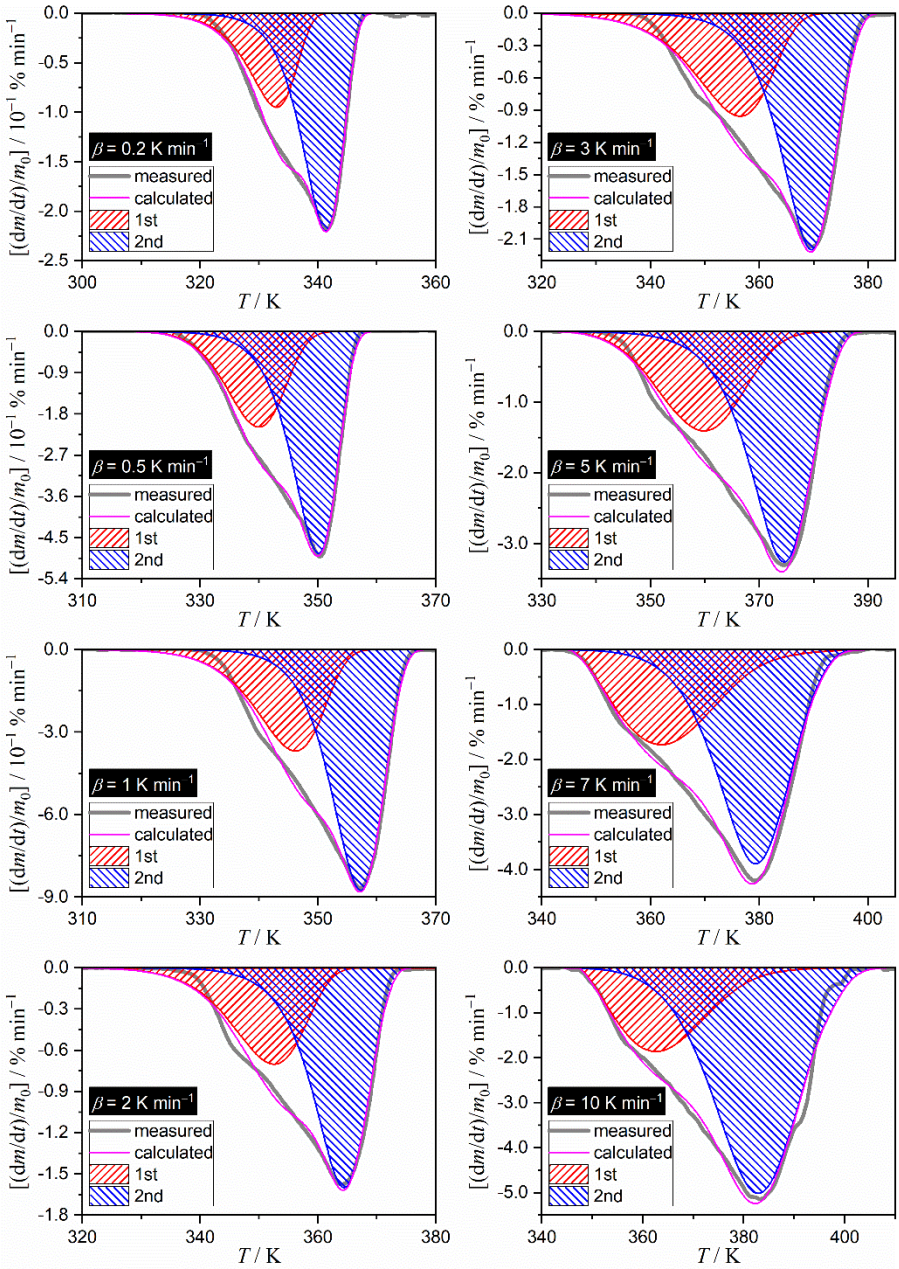

Figure S9. The results of the MDA applied to the DTG curve for the thermal dehydration of SC-MH at different β values under dry N_2 gas flow.

Table S2. The results of the MDA and subsequent formal kinetic analysis of the mathematically separated reaction steps of the thermal dehydration of SC-MH

Step i	c_i	$E_{a,i}$ / kJ mol^{-1}, [a]	$\frac{d\alpha_i}{d\theta_i} = A_i\alpha^{m_i}(1-\alpha_i)^{n_i}[-\ln(1-\alpha_i)]^{p_i}$				
			A_i / s^{-1}	m_i	n_i	p_i	R^2, [b]
1	0.36 ± 0.03	93.7 ± 14.6	(4.69 ± 0.03) × 10^{11}	0.81 ± 0.06	0.78 ± 0.02	−0.42 ± 0.05	0.9999
2	0.64 ± 0.03	83.3 ± 5.3	(5.95 ± 0.02) × 10^{9}	−0.23 ± 0.02	1.09 ± 0.01	0.84 ± 0.02	0.9999

[a] Averaged over $0.1 \le \alpha_i \le 0.9$.
[b] Determination coefficient of the nonlinear least-squares analysis for fitting the experimental master plot with SB(m, n, p) model.

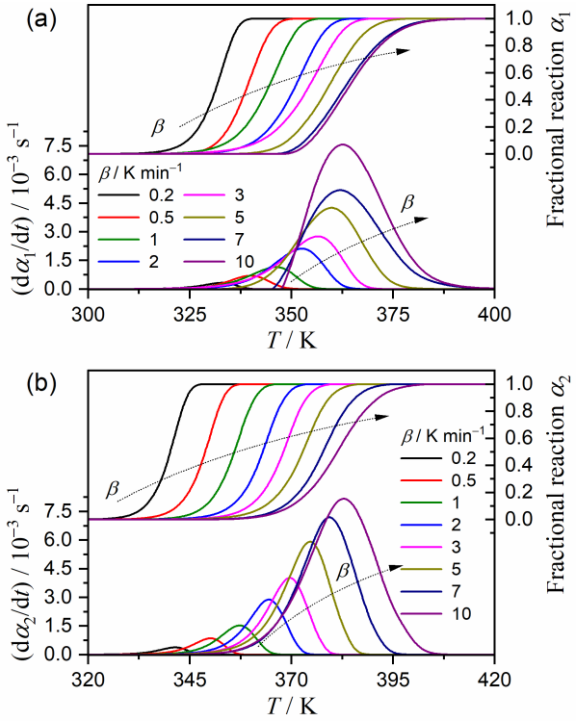

Figure S10. Kinetic curves for the two component reaction steps derived by the MDA: (a) first step (i = 1) and (b) second step (i = 2).

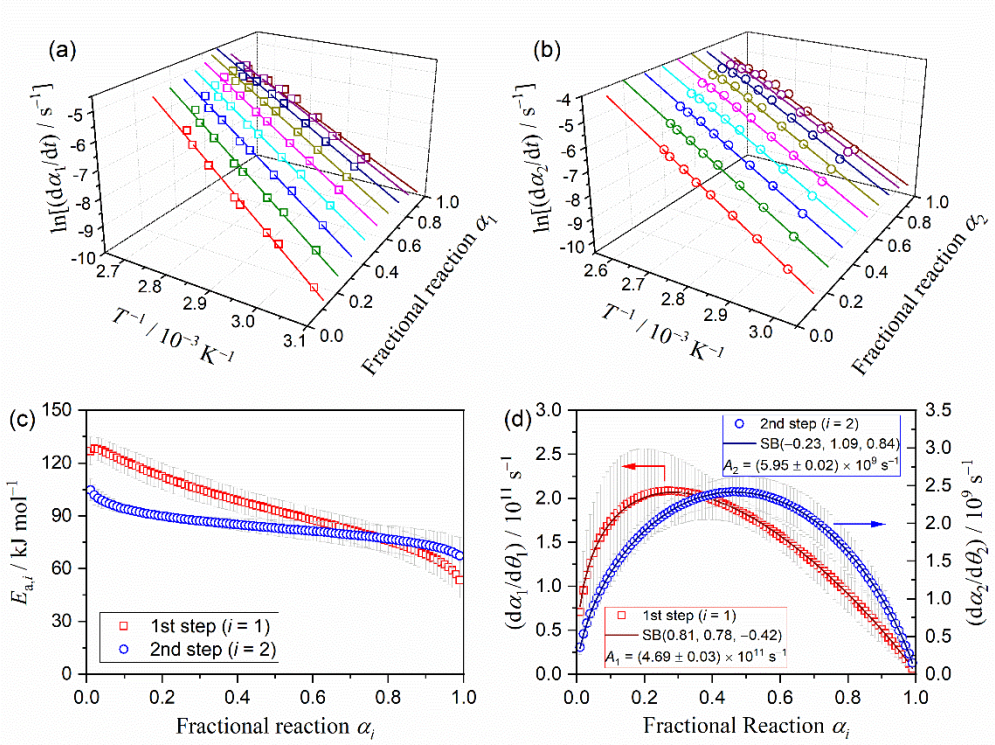

Figure S11. Isoconversional kinetic analysis for the individual reaction steps separated by the MDA: (a) Friedman plots for the first reaction step, (b) Friedman plots for the second reaction step, (c) $E_{a,i}$ values at various α_i values, and (d) experimental master plots of ($d\alpha_i/d\theta_i$) versus α_i.

S3-4. Kinetic analysis based on the SR–PBR(*n*) model

Table S3. Optimized k_{SR} and $k_{PBR(3)}$ values for the first reaction step of the thermal dehydration of SC-MH at different temperatures

T / K	k_{SR} / 10^{-4} s^{-1}	$k_{PBR(3)}$ / 10^{-4} s^{-1}	R^2
320.8	2.293	0.521	0.9987
322.7	2.511	0.641	0.9901
324.2	3.860	1.098	0.9993
326.1	5.338	1.367	0.9982
328.0	6.639	1.701	0.9966
329.9	7.406	2.046	0.9988
331.7	8.879	2.396	0.9985
334.0	7.321	5.141	0.9970
336.2	11.647	7.267	0.9975
338.1	13.289	7.672	0.9982
340.1	16.086	11.545	0.9969
341.9	19.468	13.835	0.9958
344.0	19.834	24.675	0.9900
345.9	25.452	42.651	0.9746
348.0	24.817	16.175	0.9917